J. Geodynamics Vol. 16, No. 3, pp. 147–179, 1992
Printed in Great Britain.

0264-3707/92 $5.00+0.00

RATES OF ACTIVE CRUSTAL DEFORMATION IN THE AEGEAN AND THE SURROUNDING AREA

C. B. PAPAZACHOS, A. A. KIRATZI and B. C. PAPAZACHOS

Geophysical Laboratory, University of Thessaloniki, Thessaloniki, 54006, Greece

(Received 4 November 1992)

Abstract—Active crustal deformation is calculated for 26 zones of shallow seismicity in the Aegean and the surrounding regions. The data analysis is based on a procedure developed in a previous paper (Papazachos and Kiratzi, 1993). This procedure takes advantage of all the available historical and instrumental data for the calculation of the "size" of the deformation in a seismic zone and of all reliable fault plane solutions which are available for the broader seismic belt for the determination of the "shape" of the deformation. The Aegean and its surroundings has been divided into 11 such seismic belts which may consist of one or more seismic zones that share earthquakes with similar focal mechanisms.

This data analysis showed that along the coastal region of Albania, Yugoslavia and western Greece the deformation is taken up by compression in a direction perpendicular to the coast line (47°E) at a rate of about 2 mm/a. In the Ionian islands (Leukada, Cephalonia, Zante) compression occurs at a rate of 10 mm/a in an almost EW direction (N83°E) and extension at a rate of 11 mm/a in an almost NS direction (N174°E). Along the convex side of the Hellenic arc (south of Peloponese, Crete, Rodos), the upper crust is compressed at a rate of about 6 mm/a in a direction N34°E. In the Aegean Sea and the surrounding lands (mainland of western and northern Greece, southern Yugoslavia and Bulgaria, western Turkey) the seismic deformation is taken up by an almost NS extension at an average rate of 5 mm/a. In northwestern Anatolia and the northern Aegean fault zones deformation is controlled by the westward movement along the North Anatolian fault. Northern Anatolia is undergoing a N115°E compression at a rate of 22 mm/a which is relieved by a N25°E extension at a rate of 19 mm/a, and the Northern Aegean is undergoing EW compression at a rate of 16 mm/a and NS extension at a rate of 8 mm/a.

The vertical crustal thickening along the external compressional zones ranges from 0.2 to 0.5 mm/a with an average of 0.3 mm/a and the vertical crustal thinning in the inner back-arc extensional area ranges from 0.1 to 2.4 mm/a with an average equal to 0.8 mm/a.

In the western part of the area and between the external compressional field and the internal extensional field, a belt exists where the deformation is expressed as extension at an average rate of 1.6 mm/a in a N112°E direction.

1. INTRODUCTION

The Aegean and the surrounding area is considered to be one of the seismically most active regions of the world. Destructive shallow earthquakes with M_s values up to 7.8, and intermediate depth earthquakes, with even larger magnitudes [up to 8.0, e.g. the 1926 earthquake near Rodos; Comninakis and Papazachos (1986)]

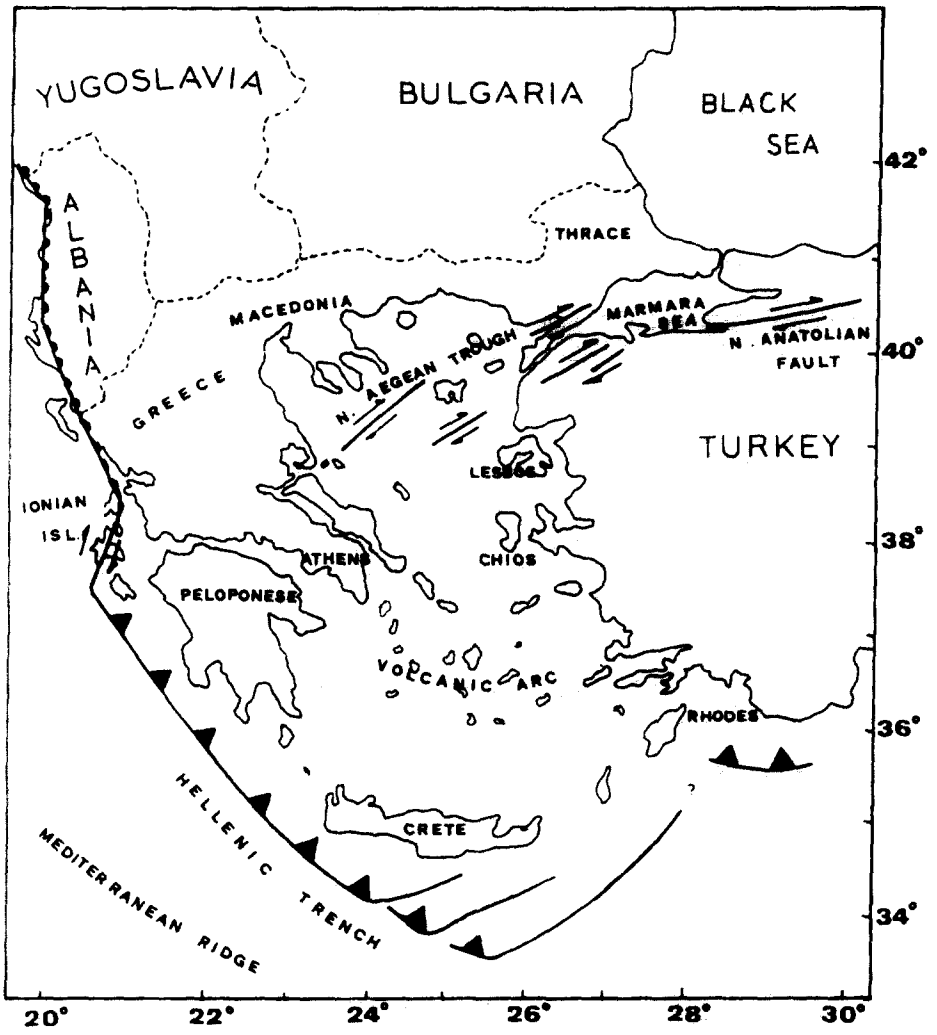

Fig. 1. Tectonic features of the Aegean area.

have repeatedly struck many sites. Therefore, a good knowledge of the geodynamics and of the accumulation of seismic strain is important from both the theoretical and the practical point of view.

In Fig. 1 the most prominent features of the Aegean area are shown. These are, from south to north, the *Mediterranean Ridge*, a compressional submarine accretionary prism of material which extends from the Ionian Sea to Cyprus and follows the trend of the Hellenic arc, the *Hellenic Trench* with a maximum water depth of 5 km, the *Hellenic arc*, which consists of the outer sedimentary arc and the inner volcanic arc, and finally the *Back-arc Aegean* area, which includes the Aegean Sea, the mainland of Greece, Albania, south Yugoslavia, south Bulgaria and western Turkey.

In the present paper, seismic crustal deformation rates are calculated for 26 seismic zones of the broader Aegean region. Previous relevant work has been

published by several researchers. Most of this work concerns the inner part of the Hellenic arc which is dominated by an extensional tectonic field of NS direction. Various values of velocity rates have been calculated that usually range between 5 and 22 mm/a (Eyidogan, 1988; Jackson and McKenzie, 1988b; Ekstrom and England, 1989; Ambraseys and Jackson, 1990; Papazachos *et al.*, 1991a; Kiratzi, 1991) but values down to 3 mm/a (Tselentis and Makropoulos, 1986) and up to 60 mm/a (Jackson and McKenzie, 1988a) have also been reported. The differences in these results are probably attributed to the data sets used and to the different moment–magnitude scaling relations.

Eyidogan (1988) calculated that deformation in the Marmara province (northwest Anatolia fault system) is expressed as right lateral shear motion of the order of 24 mm/a, while Kiratzi (1991) estimated a velocity rate of 15 mm/a of EW compression relieved by 9 mm/a of north–south extension in the northern Aegean area where right lateral strike–slip faulting also prevails. Anderson and Jackson (1987) calculated a seismic shortening of 2 mm/a in the Adriatic region along a direction normal to the coast. Along the convex side of the Hellenic arc Jackson and McKenzie (1988a) estimated a subduction rate of 100 mm/a, later reduced to 15 mm/a (Jackson and McKenzie, 1988b), while Tselentis *et al.* (1988) calculated a subduction rate of 11 mm/a along the western part of this arc.

The data analysis followed by the above mentioned authors requires the knowledge of the fault plane solution (strike, dip, rake) and of the seismic moment for each earthquake over a certain threshold magnitude and for a long enough period of time. It is true, however, that reliable fault plane solutions exist for recent strong earthquakes, so this method of analysis is only applicable to an observational period of 30 years and only to large earthquekes. Of course, it is possible to extend this period back in time, by assuming the fault parameters of the past earthquakes. On the other hand, these assumptions introduce considerable error and bias. The fact that these past events have a large magnitude has a strong impact on the results.

To overcome these drawbacks, Papazachos and Kiratzi (1993) suggested a method of analysis which permits:

(a) the use of all available complete data which include information on smaller recent shocks and on strong instrumental and historical earthquakes of a long period for the calculation of the seismic moment rate in a seismic zone, and

(b) the use of those fault parameters that are deduced from well-determined fault plane solutions of recent strong earthquakes and from good field observations of past strong earthquakes, which occurred in a broader seismic belt.

The present paper presents the results of the application of this procedure to 26 shallow seismic zones of the Aegean and its surroundings.

2. METHOD OF ANALYSIS AND DATA

The method of analysis applied in the present paper for the estimation of active crustal deformation in an area is the one proposed by Papazachos and Kiratzi (1993) which is mainly based on Kostrov's (1974), Molnar's (1979) and Jackson and McKenzie's (1988a) formulations. Initially, the "size" of the deformation, represented by the annual scalar moment rate, $\dot{M}_0$, is calculated in each zone using the following relations defined by Molnar (1979),

$$\dot{M}_0 = \frac{A}{1-B} \cdot M_{0,\max}^{1-B} \tag{1}$$

where $M_{0,\max}$ is the moment of the largest ever observed earthquake of the zone and

$$A = 10^{\left(a+\frac{bd}{c}\right)} \text{ and } B = \frac{b}{c} \tag{2}$$

where a and b are the constants of the Gutenberg–Richter relation and c and d are the constants of the moment magnitude relation:

$$\log M_0 = cM_s + d. \tag{3}$$

Then the "shape" of the deformation is defined for each seismic belt (including one or more zones of the same seismotectonic features) as described in the following.

The moment tensor M^n of the nth focal mechanism in the belt is calculated by (Aki and Richards 1980):

$$M^n = M_0^n (\bar{u} \cdot \bar{n} + \bar{u} \cdot \bar{n}) = M_0^n F^n \tag{4}$$

where M_0^n is the scalar moment of the event, $\bar{u}$ and $\bar{n}$ are the unit vectors parallel to the slip and normal to the fault plane, respectively, and $F^n = \bar{u}\cdot\bar{n} + \bar{n}\cdot\bar{u}$. We want to rewrite equation (4) for the moment rate, $\dot{M}$, of the whole belt, that is:

$$\dot{M} = \dot{M}_0 \cdot \bar{F} \tag{5}$$

where $\dot{M}_0$ is the annual scalar moment rate and $\bar{F}$ is a "representative focal mechanism tensor" of the belt. From equation (5), it is obvious that $\bar{F}$ is calculated using the following relation:

$$\bar{F} = \frac{\dot{M}}{\dot{M}_o} = \frac{\sum_{n=1}^{N} M^n / \tau}{\sum_{n=1}^{N} M_0^n / \tau} = \frac{\sum_{n=1}^{N} M^n}{\sum_{n=1}^{N} M_0^n} \tag{6}$$

where N is the number of all the available focal mechanisms which occurred in a τ time period. Since $\bar{F}$ does not depend on τ, we do not have to use a complete data set but simply all the available focal mechanisms.

The equations initially defined by Kostrov (1974) and Jackson and McKenzie (1988a) can now be transformed and the strain rate, $\dot{\varepsilon}$, and velocity, U, tensors are calculated using the following relations:

$$\dot{\varepsilon}_{ij} = \frac{1}{2\mu V} \dot{M}_0 \bar{F}_{ij} \quad i,j = 1,2,3 \tag{7}$$

$$U_{il} = \frac{1}{2\mu l_k l_j} \dot{M}_0 \bar{F}_{il} \quad i \neq k, k \neq j, j \neq i, i = 1,2,3 \tag{8}$$

$$U_{12} = \frac{1}{\mu l_1 l_2} \dot{M}_0 \bar{F}_{12} \tag{9}$$

$$U_{13} = \frac{1}{\mu l_1 l_3} \dot{M}_0 \bar{F}_{13} \tag{10}$$

$$U_{23} = \frac{1}{\mu l_1 l_3} \dot{M}_0 \bar{F}_{23} \tag{11}$$

where μ is the bulk modulus ($=3\times10^{11}$ dyn/cm^2), V is the volume of the deforming zone, l_1 and l_2 denote the length and the width of the seismic zone, respectively, while l_3 denotes the depth extend of the seismogenic layer. The reference system, $Ox_2x_2x_3$, is the zones $0l_1l_2l_3$ system. It is obvious that since $\bar{F}$ is calculated in the North–East–Down system, a rotation of $\bar{F}$ in the reference system of the zone is necessary before it is incorporated in equations (6) to (11).

The method described above requires two sets of data. The first set includes the data needed for the estimation of the seismic moment rate in each seismic zone, while the second set of data includes fault plane solutions (strike, dip, rake) and the corresponding magnitudes required for the determination of the "shape" of the deformation in each seismic belt.

The data source for the magnitudes and the epicenters of earthquakes was the catalogue of Comninakis and Papazachos (1986) for the period 1901–1985 and the monthly bulletins of the National Observatory of Athens and of the Geophysical Laboratory of the University of Thessaloniki, for the period 1986–1990. As far as historical earthquakes (before the present century) are concerned, such information was collected from the book of Papazachos and Papazachou (1989). Although this book is published in Greek it contains extensive English abstracts. In this book a catalogue of historical earthquakes and detailed information about their macroseismic effects is included. The accuracy of the magnitudes of the historical events is estimated to be of the order of 0.35 or less (Papazachos and Papazachou, 1989).

The whole area has been separated into 26 seismic zones shown in Fig. 2. This separation was mainly based on the work of Papazachos (1990). However,

the 36 seismic zones originally defined by him, were reduced to 26 because some of these zones exhibited the same pattern in terms of seismicity distribution, focal mechanisms and tectonic setting. For instance, zones 2a and 2b in Papazachos (1990) were unified in zone 2 since they represent the same type of dextral strike–slip faulting in contrast to the neighbouring zones 1c and 3, which represent thrusting. The main effort of this separation was to obtain larger zones within which the deformation is homogeneous. Nevertheless, such a zonation is strongly influenced by previous research and personal experience and certainly is not a completely objective process.

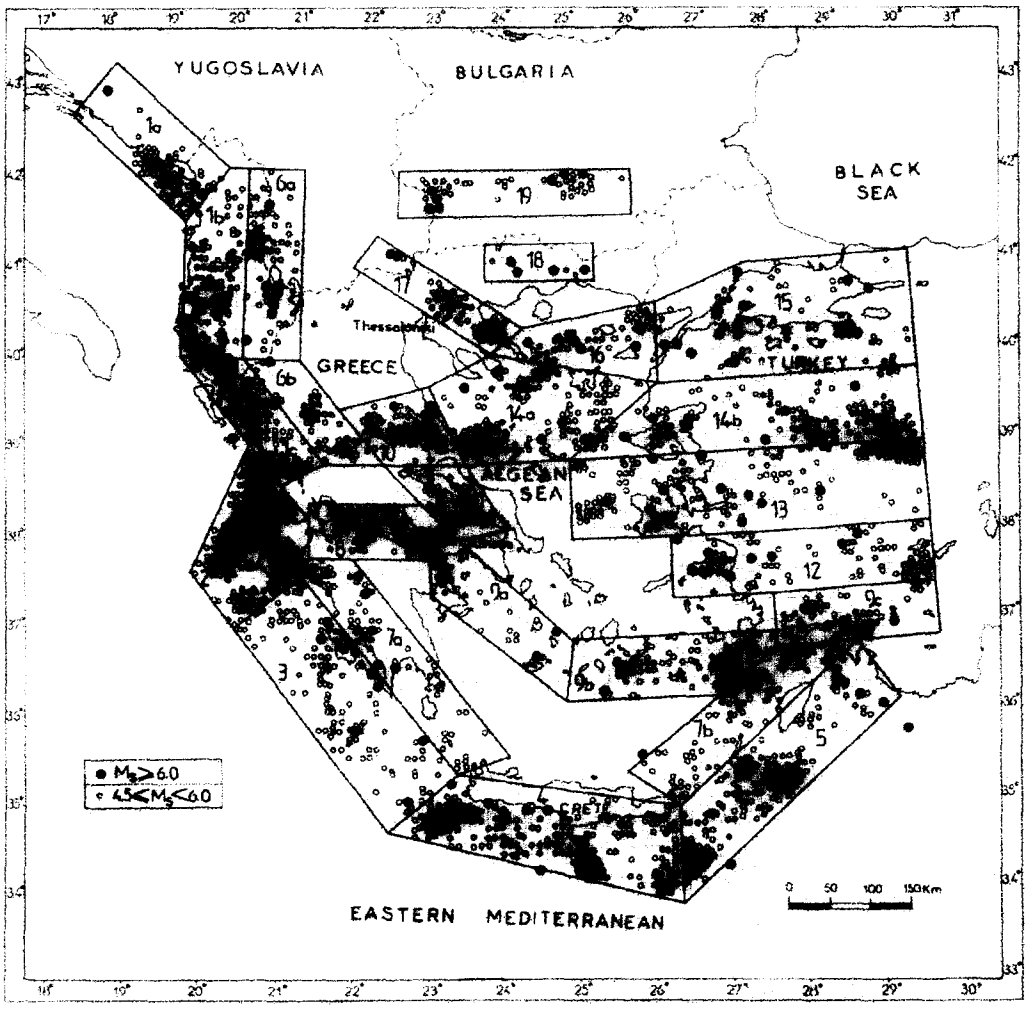

Fig. 2. The seismic zones of shallow earthquakes identified in the broader Aegean area [modified from Papazachos (1990)].

Table 1. Information on the parameters used in the calculations, for each seismic zone separately (see text for information on the notation)

Zone	t	M_{min}	ξ	M_{max}	l_1 (km)	l_2	a	b	$\dot{M}_0$ (dyncma×10^{25})
1a									
41.60, 19.40	1855	6.5	121	7.1	178	74	4.8	1.0	0.52
42.00, 20.00	1901	5.5							
41.35, 18.00	1950	5.0							
42.70, 17.60	1965	4.5							
1b									
40.10, 19.40	1833	6.2	4	6.7	204	75	4.9	1.0	0.41
40.10, 20.30	1901	5.5							
42.20, 20.30	1917	5.0							
42.20, 20.00	1965	4.5							
41.60, 19.40									
1c									
38.70, 20.90	1809	6.1	147	6.5	187	73	4.9	1.0	0.33
38.95, 21.50	1901	5.5							
40.10, 20.30	1917	5.0							
40.10, 19.40	1965	4.5							
2									
37.10, 20.30	1767	7.2	2	7.2	211	121	5.4	1.0	2.33
37.80, 21.40	1825	6.3							
38.30, 21.30	1901	5.5							
39.15, 20.45	1911	5.0							
37.70, 19.70	1965	4.5							
3									
34.85, 22.45	1866	6.5	148	7.5	307	132	5.1	1.0	1.65
35.50, 23.40	1925	5.0							
37.70, 21.20	1965	4.5							
37.10, 20.30									
4									
34.00, 26.40	1805	6.7	100	7.2	370	108	5.1	1.0	1.17
35.10, 26.40	1901	5.5							
35.50, 23.40	1919	5.0							
34.70, 22.20	1965	4.5							
5									
34.20, 26.40	1851	7.2	51	7.2	324	188	5.1	1.0	1.17
36.15, 29.45	1911	5.5							
36.80, 28.90	1919	5.0							
35.10, 26.40	1965	4.5							
6a									
40.10, 20.30	1843	6.2	174	6.7	223	66	4.7	1.0	0.26
40.10, 21.10	1901	5.5							
42.20, 21.10	1920	5.0							
42.30, 20.30	1965	4.5							
6b									
38.95, 21.50	1901	5.5	141	6.5	168	71	3.3	0.8	0.12
38.95, 22.35	1911	5.0							
40.10, 21.10	1965	4.5							
40.10, 20.30									

—continued overleaf

Table 1—*continued*

Zone	t	M_{min}	ξ	M_{max}	l_1 (km)	l_2	a	b	$\dot{M}_0$ (dyncma$\times 10^{25}$)
7a									
35.50, 23.40	1842	6.4	142	6.5	317	90	4.2	0.9	0.24
35.70, 24.10	1901	5.5							
37.90, 21.30	1911	5.0							
37.70, 21.30	1965	4.5							
7b									
35.10, 26.40	1842	6.4	54	6.8	254	82	3.6	0.8	0.38
36.80, 28.90	1911	5.0							
36.80, 27.80	1965	4.5							
35.50, 25.70									
8									
37.90, 21.30	1748	6.6	101	7.0	163	57	4.9	1.0	0.58
37.90, 23.00	1858	6.0							
38.20, 23.30	1901	5.5							
38.50, 22.90	1911	5.0							
38.50, 21.30	1965	4.5							
9a									
36.30, 24.90	1733	6.4	130	6.5	181	101	4.4	1.0	0.10
37.00, 25.00	1911	5.0							
38.20, 23.30	1965	4.5							
37.90, 23.00									
37.50, 23.00									
9b									
36.30, 24.90	1866	6.2	91	7.5	187	70	3.7	0.8	1.48
36.30, 27.00	1901	5.5							
36.80, 27.80	1911	5.0							
37.00, 27.80	1965	4.5							
37.00, 25.00									
9c									
36.80, 27.80	1869	6.8	84	6.8	191	60	4.1	0.9	0.29
36.80, 30.00	1901	5.5							
37.40, 30.00	1920	5.0							
37.40, 27.80	1965	4.5							
10									
38.95, 22.35	1901	5.5	98	7.0	119	55	3.9	0.8	1.05
38.95, 23.50	1911	5.0							
39.80, 23.00	1965	4.5							
39.55, 21.70									
11									
38.10, 23.30	1758	6.8	108	7.0	117	77	4.1	0.9	0.38
38.20, 24.10	1874	6.0							
38.95, 23.50	1901	5.5							
38.95, 22.35	1965	4.5							
12									
37.40, 26.40	1873	6.0	96	7.0	306	79	4.4	0.9	0.77
37.40, 30.00	1901	5.5							
38.10, 30.00	1918	5.0							
38.10, 26.40	1965	4.5							

—*continued opposite*

Table 1—*continued*

Zone	t	M_{min}	ξ	M_{max}	l_1 (km)	l_2	a	b	$\dot{M}_0$ dyncma×10^{25})
13									
38.10, 25.00	1845	6.2	84	6.8	425	101	4.5	0.9	0.74
38.10, 30.00	1901	5.5							
39.00, 30.00	1920	5.0							
39.00, 25.00	1965	4.5							
14a									
38.95, 23.50	1868	6.2	80	7.2	212	125	3.9	0.8	1.44
39.00, 25.00	1911	5.0							
39.80, 26.30	1965	4.5							
40.15, 23.85									
39.80, 23.00									
14b									
39.00, 25.00	1845	6.7	91	7.1	405	85	4.5	0.9	1.11
39.00, 30.00	1901	5.5							
39.80, 30.00	1920	5.0							
39.80, 26.30	1965	4.5							
15									
39.80, 26.30	1766	7.4	91	7.7	306	143	3.3	0.7	4.19
39.80, 30.00	1855	6.2							
41.10, 30.00	1901	5.5							
41.10, 27.60	1911	5.0							
40.70, 26.30	1965	4.5							
16									
39.80, 26.30	1859	6.5	77	7.5	179	42	3.1	0.7	1.83
40.70, 26.30	1971	5.5							
40.45, 24.35	1930	5.0							
40.15, 23.85	1965	4.5							
17									
40.15, 23.85	1901	5.5	124	7.0	155	40	3.2	0.7	0.92
40.45, 24.35	1911	5.0							
41.50, 22.20	1965	4.5							
41.10, 22.00									
18									
41.00, 23.80	1784	6.0	102	7.3	114	37	2.4	0.7	0.25
41.00, 25.40	1901	5.5							
41.40, 25.40	1911	5.0							
41.40, 23.80	1965	4.5							
19									
41.70, 22.50	1750	6.8	84	7.7	242	39	2.5	0.7	0.67
41.70, 26.00	1901	5.5							
42.20, 22.50	1965	4.5							

Table 1 gives information on the parameters of each seismic zone. A code number is given to each seismic zone (1a, 1b, 1c, 2...). The first two columns list the coordinates defining the limits of the seismic zone. The third column gives the date since when the data are complete for a certain magnitude which is listed in the fourth column. For example, for the first zone, 1a, the complete

data groups are all shallow earthquakes with $M_s \geq 6.5$, 5.5, 5.0 and 4.5 for the periods 1855–1990, 1901–1990, 1950–1990 and 1965–1990, respectively. The fifth column lists the azimuth of the zone's principal direction while the sixth column gives the maximum magnitude ever observed in each one. The seventh and eighth columns list the length and the width of each deforming zone, determined in a way described in the text to follow. The ninth and tenth columns list the a and b parameters, of the Gutenberg–Richter relation, respectively. Finally, the last column of Table 1 lists the value of the seismic moment rate for each seismic zone, determined using equations (1), (2) and (3). The values $c=1.5$, $d=15.89$ (Papazachos and Kiratzi, 1993) were used in the calculation of the annual scalar moment rate. The values of a and b of the Gutenberg–Richter relation were calculated for each seismic zone by a method known as "mean value" method (Milne and Davenport, 1969) which is described in detail by Papazachos (1990).

Figure 2 also shows the epicenters of the earthquakes, of the complete groups of data, for all 26 seismic zones here examined. As it is seen in this figure, in some cases the area covered by epicenters does not necessarily cover the whole seismic zone. Since we are interested in the active part of each zone and because for the purpose of the present paper we need to have zones of rectangular shape, we assumed that the epicentral area of each zone has such shape. Thus, the length, the width and the azimuth of each zone were calculated as follows: using the complete data set we calculated the coordinates of the center of the zone which we chose as the center of a coordinate system with x and y axes parallel to NS and EW direction, respectively. Assuming that the earthquakes in each zone generally follow a linear pattern, we calculated a least squares' best fit line for each zone. The azimuth, ξ, is taken to be the azimuth of the line with the North. The projections of the most distant epicenters, from the center of the zone, onto this line define the length, l_1, of the zone. The width, l_2, of the zone is taken to be 4σ, where σ is the standard deviation of the earthquake epicenters from the line. The value of l_3 (depth extent of the seismogenic layer) was taken to be 15 km from all zones of shallow seismicity. This is not a crude assumption since the inversion of mainly body wave studies of the shallow earthquakes of the Aegean revealed that this seismicity is nucleated at the upper 15 km of the crust (Anderson and Jackson, 1987; Ioannidou, 1989; Kiratzi and Langston, 1991; Kiratzi *et al.*, 1991a, b; Taymaz *et al.*, 1991).

Table 2 gives information on all the focal mechanisms (strike, dip and rake) used in this analysis. The main data source for the fault plane solutions was the catalogue published by Papazachos *et al.* (1991b). All fault plane solutions listed in Table 2 are accordingly referenced. The focal mechanisms of three past earthquakes (Nos 79, 80 and 81 in Table 2), were compiled during this study on the basis of extensively reported field observations (Papazachos and Papazachou, 1989).

The seismic zones have been grouped in 11 seismic belts of similar fault plane solutions and the "shape" tensor, $\bar{F}$, of each belt has been determined by means of the available fault plane solutions of the corresponding belt.

Table 2. Fault plane parameters for the shallow ($h \leq 40$ km) earthquakes of the Aegean and surrounding area. The data cover the period 1963–1986 with $M_s \geq 5.5$. Data for four older events (Nos 1, 79, 80, 81) are also included

No.	Date	Zone	Origin time	Epicentral coordinates		Nodal plane 1			M_s	Ref.
				Lat °N	Lon °E	strike °	dip °	rake °		
1	9 July 1956	9b	03:11:40	36.7	25.8	65	40	−90	7.5	1
2	26 July 1963	17	04:17:12	42.0	21.4	322	73	−20	6.1	2
3	18 Sep. 1963	15	16:58:08	40.8	29.1	277	72	−94	6.3	2
4	16 Dec. 1963	3	13:47:53	37.0	21.0	286	16	90	5.9	3
5	6 Oct. 1964	15	14:31:23	40.3	28.2	273	46	−95	6.9	4
6	9 Mar. 1965	14a	17:57:54	39.3	23.8	40	90	−6	6.1	2
7	5 Apr. 1965	8	03:12:55	37.7	22.0	226	57	−159	6.1	2
8	27 Apr. 1965	7a	14:09:06	35.6	23.5	22	27	−81	5.7	5
9	13 June 1965	12	20:01:51	37.8	29.3	259	38	−90	5.6	4
10	6 July 1965	11	03:18:42	38.4	22.4	270	14	−90	6.3	2
11	5 Feb. 1966	10	02:01:45	39.1	21.7	103	23	−75	6.2	6
12	9 May 1966	4	00:42:53	34.4	26.4	295	40	90	5.8	2
13	29 Oct. 1966	1c	02:39:25	38.9	21.1	335	27	132	6.0	6
14	4 Mar. 1967	14a	17:58:09	39.2	24.6	98	54	−107	6.6	2
15	1 May 1967	6b	07:09:02	39.5	21.2	2	36	−100	6.4	4
16	30 Nov. 1967	6a	07:23:50	41.4	20.4	0	33	−107	6.3	6
17	19 Feb. 1968	14a	22:45:42	39.4	24.9	217	86	175	7.1	7
18	28 Mar. 1968	2	07:39:59	37.8	20.9	354	34	137	5.9	6
19	30 May 1968	5	17:40:26	35.4	27.9	293	25	90	5.9	2
20	5 Dec. 1968	9b	07:52:11	36.6	26.9	86	50	−90	5.9	2
21	14 Jan. 1969	5	23:12:06	36.1	29.2	282	25	95	6.2	2
22	3 Mar. 1969	15	00:59:10	40.1	27.5	221	64	41	6.0	2
23	23 Mar. 1969	14b	21:08:42	39.1	28.5	70	46	−128	6.1	2
24	25 Mar. 1969	14b	13:21:34	39.2	28.4	90	40	−105	6.0	2
25	28 Mar. 1969	13	01:48:29	38.5	28.5	281	28	−90	6.6	2
26	3 Apr. 1969	1b	22:12:22	40.7	20.0	143	30	90	5.8	14
27	6 Apr. 1969	13	03:49:34	38.5	26.4	280	30	−90	5.9	2
28	16 Apr. 1969	5	23:21:06	35.2	27.7	301	30	109	5.5	2
29	12 June 1969	4	15:13:31	34.2	25.0	294	29	105	6.1	2
30	8 July 1969	2	08:09:13	37.5	20.3	354	18	115	5.9	3
31	13 Oct. 1969	1c	01:02:31	39.8	20.6	340	30	160	5.8	6
32	28 Mar. 1970	14b	21:02:23	39.2	29.5	280	30	−90	7.1	4
33	28 Mar. 1970	14b	23:11:43	39.1	29.6	73	32	−109	5.5	8
34	8 Apr. 1970	8	13:50:28	38.3	22.6	278	20	−85	6.2	15
35	16 Apr. 1970	14b	10:42:22	39.0	29.9	273	30	−99	5.7	8
36	19 Apr. 1970	14b	13:29:36	39.0	29.8	102	23	−90	6.0	8
37	23 Apr. 1970	14b	09:01:27	39.1	28.6	265	40	−83	5.6	8
38	19 Aug. 1970	1b	02:01:52	41.1	19.8	343	20	90	5.4	2
39	12 May 1971	12	06:25:15	37.6	29.7	68	40	−90	6.2	4
40	12 May 1971	12	10:10:38	37.6	29.7	73	14	−90	5.6	4
41	12 May 1971	12	12:57:25	37.6	29.6	79	22	−72	5.7	4
42	25 May 1971	14b	05:43:26	39.0	29.7	97	40	−101	6.1	8
43	14 Mar. 1972	14b	14:05:47	39.3	29.5	101	40	−101	5.6	8
44	4 May 1972	4	21:39:57	35.1	23.6	308	18	90	6.5	9
45	17 Sep. 1972	2	14:07:15	38.3	20.3	46	66	−174	6.3	3
46	5 Jan. 1973	3	05:49:18	35.8	21.9	306	30	82	5.6	3
47	4 Nov. 1973	2	15:52:13	38.9	20.5	348	40	109	5.8	6
48	29 Nov. 1973	4	10:57:44	35.2	23.8	316	10	90	6.0	8
49	27 Mar. 1975	16	05:15:08	40.4	26.1	41	60	−128	6.6	8
50	11 May 1976	2	16:59:45	37.4	20.4	327	12	90	6.5	3
51	12 June 1976	2	00:59:18	37.5	20.6	297	20	90	5.8	6
52	18 Aug. 1977	4	09:27:41	35.3	23.5	270	12	114	5.6	10
53	11 Sep. 1977	4	23:19:19	34.9	23.0	320	30	90	6.3	4

—continued overleaf

Table 2—*continued*

No.	Date	Zone	Origin time	Epicentral coordinates Lat °N	Lon °E	Nodal plane 1 strike °	dip °	rake °	M_s	Ref.
54	23 May 1978	17	23:34:11	40.7	23.2	227	49	−64	5.8	11
55	20 June 1978	17	20:03:21	40.8	23.2	278	46	−70	6.5	11
56	15 Apr. 1979	1a	06:19:41	42.0	19.0	318	12	90	7.1	12
57	15 May 1979	4	06:59:23	34.6	24.5	253	17	65	5.7	10
58	24 May 1979	1a	17:23:18	42.2	18.8	330	22	90	6.3	12
59	14 June 1979	13	11:44:45	38.8	26.6	121	42	−50	5.9	2
60	23 July 1979	—	11:41:55	35.5	26.4	61	35	−40	5.5	21
61	9 July 1980	10	02:10:20	39.3	22.9	82	42	−79	5.6	13
62	9 July 1980	10	02:11:57	39.3	22.9	81	40	−90	6.5	13
63	9 July 1980	10	02:35:52	39.2	22.6	81	40	−90	6.1	13
64	24 Feb. 1981	8	20:53:37	38.2	23.0	290	44	−60	6.7	23
65	25 Feb. 1981	8	02:35:54	38.2	23.1	252	43	−104	6.4	23
66	4 Mar. 1981	8	21:58:07	38.2	23.3	60	50	−90	6.4	23
67	19 Dec. 1981	14a	14:10:51	39.2	25.2	37	67	−166	7.2	16
68	27 Dec. 1981	14a	17:39:13	38.9	24.9	212	85	−174	6.5	16
69	18 Jan. 1982	14a	19:27:25	39.8	24.4	235	50	153	7.0	16
70	17 Aug. 1982	—	22:22:20	33.7	22.9	230	45	109	6.4	10
71	17 Jan. 1983	2	12:41:30	38.1	20.2	40	45	168	7.0	17
72	23 Mar. 1983	2	23:51:05	38.2	20.3	29	68	174	6.2	17
73	5 July 1983	15	12:01:27	40.3	27.2	248	70	−155	6.1	18
74	6 Aug. 1983	16	15:43:52	40.0	24.7	48	83	178	6.8	19
75	21 June 1984	3	10:43:46	35.4	23.3	305	24	104	6.2	14
76	21 Apr. 1985	3	08:49:42	35.7	22.2	269	36	71	5.6	22
77	30 Apr. 1985	10	18:14:13	39.3	22.8	77	50	−105	5.8	23
78	13 Sep. 1986	7a	17:24:34	37.1	22.2	200	50	−8	6.0	20
79	26 Sep. 1932	17	19:20:42	40.5	23.9	90	40	−90	7.0	24
80	18 Apr. 1928	19	19:22:48	42.2	25.0	270	40	−90	7.0	24
81	18 Mar. 1953	15	19:06:16	40.0	27.4	250	70	−160	7.4	24

[1]Shirokova (1972), [2]McKenzie (1972), [3]Papadimitriou (1992), [4]Papazachos *et al.* (1991b), [5]Lyon-Caen *et al.* (1988), [6]Anderson and Jackson (1987), [7]Kiratzi *et al.* (1991a), [8]McKenzie (1978), [9]Kiratzi and Langston (1989), [10]Taymaz *et al.* (1990), [11]Soufleris and Stewart (1981), [12]Boore *et al.* (1981), [13]Papazachos *et al.* (1983), [14]Ritsema (1974), [15]Liotier (1989), [16]Papazachos *et al.* (1984b), [17]Scordilis *et al.* (1985), [18]Dziewonski *et al.* (1984), [19]Rocca *et al.* (1985), [20]Papazachos *et al.* (1988), [21]Ekstrom and England (1989), [22]NEIS, [23]Taymaz *et al.* (1991), [24]This study [based on information by Papazachos and Papazachou (1989)].

Figure 3 shows the fault plane solutions of the earthquakes listed in Table 2. The date of each earthquake is written right next to each solution. The solutions of the historical events listed with numbers 79, 80 and 81 in Table 2 are not shown in this figure.

In the following the calculated rates of deformation are given and discussed for each seismic belt.

3. RATES OF ACTIVE CRUSTAL DEFORMATION

Following the methodology described above, the rates of seismic deformation were calculated for each zone. The results are presented for each of the 11

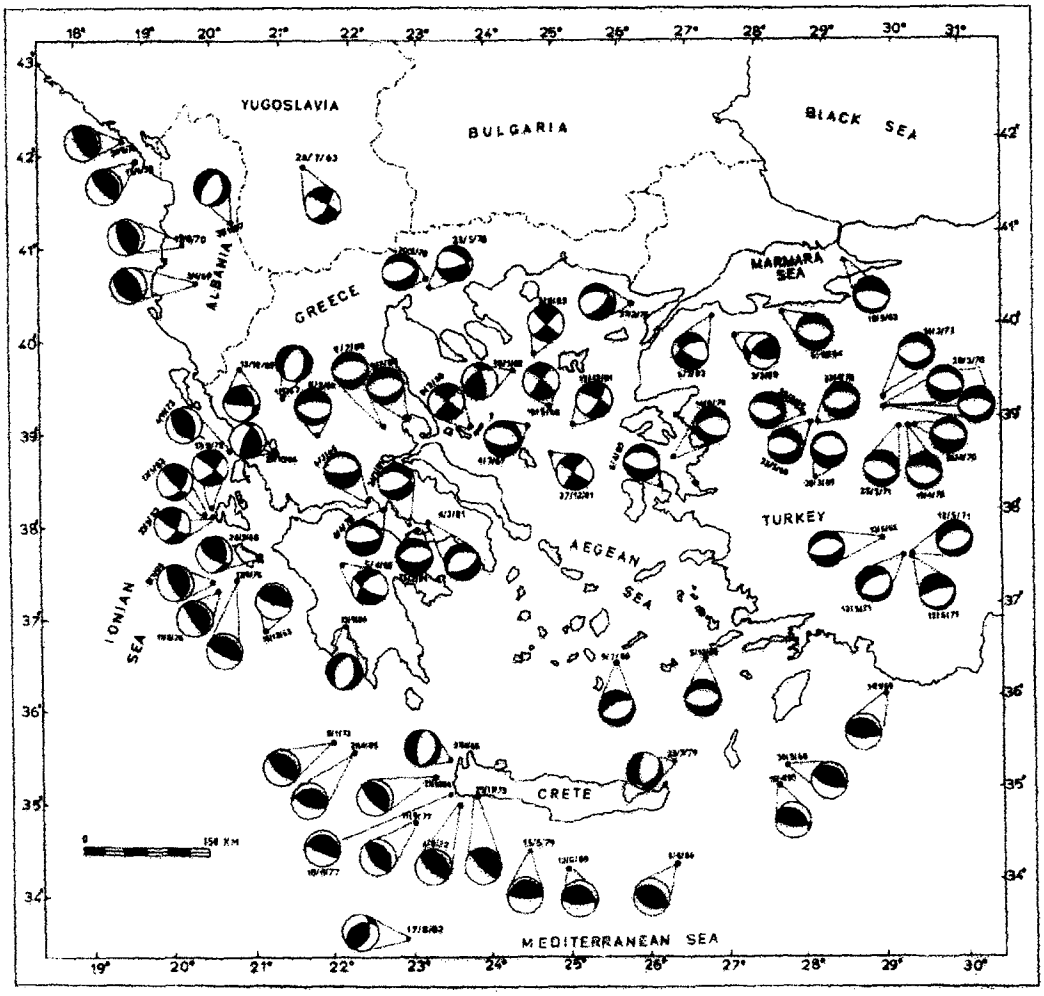

Fig. 3. Fault plane solutions for shallow earthquakes in the Aegean and the surrounding area of the period 1956–1987 [modified from Papazachos *et al.* (1991b)].

belts, separately. At first, the components of the tensor $\bar{F}$ for the whole seismic belt are given and then the components of the strain rate and velocity tensor for each seismic zone of the belt are presented.

Belt 1: Coast of Yugoslavia, Albania, Western Greece

It includes seismic zones 1a, 1b and 1b (Fig. 1). Six fault plane solutions were used in the calculations, those listed with numbers 13, 26, 31, 38, 56 and 58 in Table 2. These earthquakes show thrust faulting with the fault plane parallel to the coast. They are produced by compressional forces due to the collision of two continental lithospheres, the Apulian and the Eurasian, without any evidence of subduction.

The components of the tensor $\bar{F}$ [equation (4)] for the whole seismic belt are as follows:

−0.19	−0.22	0.59
−0.22	−0.24	0.65
0.59	0.65	0.43

The moment rate tensor, $\dot{M}$, for each zone is calculated by multiplication of the tensor $\bar{F}$ with the corresponding value of the moment rate, $\dot{M}_0$, listed in Table 1, and is not presented here. In the following, the strain rate tensor and the velocity tensor for each seismic zone, included in this seismic belt, are presented:

Zone 1a: This zone covers the southern Dalmatian coast which was struck in 1979 by the Monte Negro sequence of earthquakes (M=7.1). The elements of the strain rate tensor in the coordinate system 1: North, 2: East, 3: Down, which is adopted throughout this paper, have as follows:

−0.83	−0.96	2.61
−0.96	−1.08	2.86×10^{-8}/a
2.61	2.86	1.91

The elements of the velocity tensor in the same coordinate system are:

−0.29	−0.82	0.78
−0.82	−1.27	0.86 mm/a
0.78	0.86	0.29

while its eigenvectors are:

v (mm/a)	Azimuth°	Plunge°
−2.25	58	−24
0.10	140	16
0.87	20	60

Positive eigenvalues represent dilatation (extension or thickening) while negative ones represent compression (shortening or thinning). Positive or negative plunge means that the eigenvector is directed into or out of the solid earth, respectively.

Zone 1b: This zone extends along the western coast of Albania. The components of the strain rate tensor are as follows:

−0.56	−0.65	1.77
−0.65	−0.73	1.94×10^{-8}/a
1.77	1.94	1.29

while the velocity tensor is:

−1.19	−1.04	0.53
−1.04	−0.63	0.58 mm/a
0.53	0.58	0.19

and its eigenvectors are:

v (mm/a)	Azimuth°	Plunge°
−2.24	39	−18
0.12	135	−21
0.49	91	62

Zone 1c: This zone extends along the north-western coast of Greece. The components of the strain rate tensor are as follows:

−0.50	−0.58	1.59
−0.58	−0.65	1.73×10^{-8}/a
1.59	1.73	1.16

while the velocity tensor obtained is:

−0.49	−0.47	0.48
−0.47	−0.37	0.52 mm/a
0.48	0.52	0.17

The eigensystem of the velocity matrix is as follows:

v (mm/a)	Azimuth°	Plunge°
−1.25	43	−26
0.03	136	−7
0.53	59	63

It is seen that the deformation in belt 1 is mainly taken up by an average shortening of 1.9±0.5 mm/a, where 0.5 is the standard deviation, in a mean direction N47°±8°E, which is approximately perpendicular to the coast. These values are consistent with the results of Anderson and Jackson (1987).

Belt 2: Ionian islands

It includes only the seismic zone 2. Eight fault plane solutions were used in the calculations, listed with numbers 18, 30, 45, 47, 50, 51, 71 and 72 in Table 2. Most of them show mainly thrust faulting except for three of them in the central part of the zone which are of strike–slip type with a thrust component. The elements of the tensor $\underline{\underline{F}}$ for this seismic belt are:

0.49	−0.07	0.50
−0.07	−0.73	0.46
0.50	0.46	0.23

Zone 2: The elements of the strain rate tensor are:

5.00	−0.76	5.06
−0.76	−7.38	4.65×10^{-8}/a
5.06	4.65	2.37

while the elements of the velocity matrix have as follows:

10.6	−2.19	1.52
−2.19	−9.00	1.39 mm/a
1.52	1.39	0.36

The eigensystem of the velocity matrix is:

v (mm/a)	Azimuth°	Plunge°
11.02	174	−7
−9.50	83	−9
0.43	123	78

It is seen that almost NS extension (N174°E) at a rate of 11.0 mm/a and almost EW compression (N83°E) at a rate of 9.5 mm/a are the dominant modes of deformation in this zone. These almost horizontal deformation modes are expressed by the existence of strike–slip faults as those of the 1983 Cephalonia sequence.

Belt 3: Convex side of the Hellenic arc

It includes seismic zones 3, 4 and 5. Fourteen fault plane solutions were used in the calculations, listed with numbers 4, 12, 19, 21, 28, 29, 44, 46, 48, 52, 53, 57, 75 and 76, all representing thrust faulting. The elements of the tensor for the whole seismic belt are as follows:

−0.50	−0.27	0.57
−0.27	−0.20	0.31
0.57	0.31	0.69

Zone 3: This zone covers the western part of the Hellenic arc and extends from the western coast of Peloponese up to the western corner of Crete. The elements of the strain rate tensor are:

−2.25	−1.20	2.60
−1.20	−0.89	1.39×10^{-8}/a
2.60	1.39	3.13

while the elements of the velocity tensor are:

−5.29	−1.63	0.78
−1.63	−0.21	0.42 mm/a
0.78	0.42	0.47

and the eigenvectors are:

v (mm/a)	Azimuth°	Plunge°
−5.89	17	−8
0.19	110	−24
0.67	90	65

Zone 4: This zone covers the southern part of the Hellenic arc. The elements of the strain rate tensor are:

−1.60	−0.86	1.86
−0.86	−0.63	1.00×10^{-8}/a
1.86	1.00	2.24

The components of the velocity tensor are:

−1.52	−1.41	0.56
−1.41	−1.85	0.30 mm/a
0.56	0.30	0.34

while its eigensystem is:

v (mm/a)	Azimuth°	Plunge°
−3.21	48	−10
−0.33	135	15
0.50	168	−72

Zone 5: This zone extends from the eastern coast of Crete up to the coast of southwestern Turkey. The components of the strain rate tensor are:

−1.82	−0.98	2.11
−0.98	−0.72	1.13×10^{-8}/a
2.11	1.13	2.55

while the matrix of the velocity tensor is as follows:

−4.57	−3.45	0.63
−3.45	−2.74	0.34 mm/a
0.63	0.34	0.38

and its eigenvectors are:

v (mm/a)	Azimuth°	Plunge°
−7.30	37	−5
−0.11	126	12
0.47	151	−77

It is seen that the belt as a whole is characterized by an average compression of 5.5±1.7 mm/a in a mean direction N34°±13°E. This value almost equals the 6 mm/a that Jackson and McKenzie (1988b) calculated by using data only from shallow earthquakes. These rates of shortening, however, are too small to account for the convergence rate expressed from plate motions.

Belt 4: Eastern Albania–Central Greece

This belt has been first identified by Papazachos *et al.* (1984a). It strikes in an about north–south direction and includes seismic zones 6a, 6b and 7a. Four

fault plane solutions were used in this belt listed with numbers 8, 15, 16 and 78 in Table 2, which show normal faulting. The components of the tensor $\bar{F}$ for the whole siesmic belt are:

0.01	−0.16	0.18
−0.16	0.90	−0.32
0.18	−0.32	−0.91

Zone 6a: This zone extends along the western borders of Albania with Yugoslavia and Greece. The components of the strain rate tensor are:

0.02	−0.31	0.36
−0.31	1.79	-0.64×10^{-8}/a
0.36	−0.64	−1.82

while the velocity tensor is as follows:

0.01	−0.54	0.11
−0.54	1.24	−0.19 mm/a
0.11	−0.19	−0.03

The eigensystem configuration revealed the following values:

v (mm/a)	Azimuth°	Plunge°
1.48	112	−7
−0.10	23	8
−0.30	161	79

Zone 6b: This zone is located in the western part of central Greece. The elements of the strain rate tensor are:

0.01	−0.17	0.20
−0.17	0.99	-0.35×10^{-8}/a
0.20	−0.35	−1.01

and the velocity tensor is:

−0.01	−0.47	0.06
−0.47	1.28	−0.11 mm/a
0.06	−0.11	−0.15

its eigensystem being as follows:

v (mm/a)	Azimuth°	Plunge°
1.44	108	−4
−0.19	14	−41
−0.14	23	49

Zone 7a: This zone extends mainly along the western part of Peloponese. The most recent earthquake that occurred is the 13 September 1986 event with

a large impact on the city of Kalamata. The strain rate tensor for this zone is:

0.01	−0.15	0.17
−0.15	0.86	-0.31×10^{-8}/a
0.17	−0.31	−0.87

while the velocity tensor is:

0.29	−0.76	0.05
−0.76	1.56	−0.09 mm/a
0.05	−0.09	−0.13

and its eigensystem is:

v (mm/a)	Azimuth°	Plunge°
1.92	115	−3
−0.06	25	6
−0.14	179	83

The dominant feature of this belt, which lies between the external compressional area and the internal extensional one, is an extension with an average of 1.6±0.2 mm/a in a mean direction N112°±3°. There is no model which satisfactorily explains this almost EW extension. It is probably a side effect of the compressional stress which is exerted along the western coast of Greece. There is evidence that this EW extension extends up to the northeastern coast of Crete. The CMT solution of the event of 23 July 1979 (Ekstrom and England, 1989), and the focal mechanisms for some microearthquakes (Hatzfeld *et al.*, 1990) support this assumption. In any case, we decided not to include the solution of the event of 23 July 1979 in the calculations, because of its small magnitude.

Belt 5: *Central Greece*

It includes zones 8, 10 and 11. Ten fault plane solutions were used in the calculation listed with numbers 10, 11, 34, 61, 62, 63, 64, 65, 66 and 77 in Table 2. All solutions show normal faulting in mainly EW striking planes. The components of the tensor $\bar{F}$ for the whole seismic belt are as follows:

0.83	−0.18	−0.07
−0.18	0.08	0.05
−0.07	0.05	−0.91

Zone 8: It is located along the area of Patraikos and Corinthiakos gulfs. The most recent earthquakes that struck the region are the 1981 Alkyonides Gulf sequence. The components of the strain rate tensor are:

5.53	−1.21	−0.47
−1.21	0.51	0.35×10^{-8}/a
−0.47	0.35	−6.04

while the velocity tensor is:

3.63	−2.01	−0.14
−2.01	1.03	0.10 mm/a
−0.14	0.10	−0.91

Its eigenvectors are:

v (mm/a)	Azimuth°	Plunge°
4.73	152	2
−0.06	61	2
−0.91	109	−88

Zone 10: This zone covers the area of Thessalia. The most recent earthquakes (Ms=6.5) occurred there in the summer of 1980 (Volos sequence). The area has a long record of seismicity and has suffered many casualties. The strain rate tensor is calculated to be:

12.74	−2.78	−1.09
−2.78	1.17	0.80×10^{-8}/a
−1.09	0.80	−13.91

The velocity tensor is as follows:

7.63	−3.94	−0.33
−3.94	1.35	0.24 mm/a
−0.33	0.24	−2.09

and its eigensystem is:

v (mm/a)	Azimuth°	Plunge°
9.54	154	2
−0.54	64	3
−2.10	100	−87

Zone 11: This zone covers part of central Greece and part of western Evia. In this zone the major neotectonic fault of Atalanti controls the deformation pattern of the region. The strain rate tensor is as follows:

3.58	−0.78	−0.31
−0.78	0.33	0.22×10^{-8}/a
−0.31	0.22	−3.90

The velocity tensor is as follows:

3.50	−1.72	−0.09
−1.72	−0.06	0.07 mm/a
−0.09	0.07	−0.59

and in terms of the eigensystem configuration we have:

ν (mm/a)	Azimuth°	Plunge°
4.19	158	1
−0.76	68	−9
−0.58	60	81

It is seen that extension with an average value of 6.2±2.4 mm/a in a mean direction N155°±2°E dominates the area covered by this belt. It has to be emphasized that the deformation rates calculated in the present paper involve the seismic part of it and do not deal with the anelastic part. Billiris *et al.* (1991) calculated the total strain in central Greece on the basis of geodetic measurements. They found an almost north–south extension across the network equal to about 11 mm/a. This is about a factor of two larger than the value calculated in this work. So, for this part one may conclude that seismic strain rate makes up 50%, or so, of the total strain.

Belt 6: volcanic arc

It includes zones 9a, 9b and 7b. Two fault plane solutions were used in the calculations, listed with numbers 1 and 20 in Table 2. It is observed that there is a lack of focal mechanisms in zone 9a and 7b. Zone 9a is a zone of very low seismicity. However, since this zone is the westernmost part of the volcanic arc, we assumed that it exhibits the same deformation behaviour as the eastern part of the volcanic arc. The same assumption was made for zone 7b which lies between the eastern inner volcanic arc and the outer sedimentary arc. The components of the tensor $\bar{F}$ for this seismic belt are:

0.81	−0.38	0.16
−0.38	0.17	−0.07
0.16	−0.07	−0.98

Zone 9a: This zone forms the western part of the volcanic arc. The strain rate tensor is:

0.51	−0.24	0.10
−0.24	0.11	-0.05×10^{-8}/a
0.10	−0.05	−0.62

The velocity tensor is:

0.90	−0.48	0.03
−0.48	0.11	−0.01 mm/a
0.03	−0.01	−0.09

and the eigensystem is:

v (mm/a)	Azimuth°	Plunge°
1.15	155	−2
−0.11	65	0
−0.09	57	9

Zone 9b: This zone forms the eastern part of the volcanic arc with the great volcanoes of Thira and Nisyros. In 1956 a great earthquake occurred (Ms=7.5) near the island of Amorgos that generated a tsunami of 25 m at the northeastern part of the island. The strain rate tensor has the form:

10.29	−4.77	1.98
−4.77	2.22	-0.93×10^{-8}/a
1.98	−0.93	−12.52

The velocity tensor is:

7.31	−6.83	0.59
−6.83	4.26	−0.28 mm/a
0.59	−0.28	−1.87

and the eigensystem is:

v (mm/a)	Azimuth°	Plunge°
12.81	141	−2
−1.18	52	12
−1.94	40	−78

Zone 7b: This zone is located in the inner eastern part of the Hellenic arc. The strain rate tensor is:

1.64	−0.76	0.32
−0.76	0.36	-0.15×10^{-8}/a
0.32	−0.15	−2.00

The velocity tensor is:

1.70	−0.46	0.09
−0.46	0.08	−0.04 mm/a
0.09	−0.04	−0.30

and in terms of eigenvectors we have:

v (mm/a)	Azimuth°	Plunge°
1.83	165	−3
−0.05	75	−4
−0.31	109	85

The results show that the whole belt of the volcanic arc is characterized by an extensional field in a mean direction of N154°±10°E. The deformation velocity is 1–2 mm/a in the western part of the volcanic arc (zone 9a) and in zone 7b

but it is almost one order of magnitude larger (13 mm/a) in the eastern part of the volcanic arc (zone 9b). This is probably connected to the existence of major volcanoes in the eastern part of the arc. Papazachos and Panagiotopoulos (1993) found that the shallow seismic activity connected to the volcanic arc clusters around five volcanic centers. The majority of this seismicity is concentrated near the islands of Thira and Nisyros. Moreover, the seismic activity exhibits a linear pattern in a direction N59°E which is the mean strike of the major faults of the volcanic arc. It is interesting to see that the direction of the deformation velocity determined in the present paper (N154°E) is normal to the strike of these faults.

Belt 7: Samos–Southwestern Turkey

It includes zones 9c and 12. Four fault plane solutions are used in the calculations, listed with numbers 9, 39, 40 and 41 in Table 2. The components of the tensor $\bar{F}$ for this belt are:

0.79	−0.30	0.24
−0.30	0.11	−0.12
0.24	−0.12	−0.90

Zone 9c: This zone is located in the southern edge of Turkey. The strain rate tensor is:

2.26	−0.85	0.70
−0.85	0.32	-0.33×10^{-8}/a
0.70	−0.33	−2.59

The velocity tensor is:

1.27	−0.84	0.21
−0.84	0.47	−0.10 mm/a
0.21	−0.10	−0.39

The eigenvectors are:

ν (mm/a)	Azimuth°	Plunge°
1.82	148	−6
−0.05	58	4
−0.41	5	−83

Zone 12: This zone includes the island of Samos and southwestern Turkey. The strain rate tensor for this zone is:

2.78	−1.05	0.86
−1.05	0.40	-0.41×10^{-8}/a
0.86	−0.41	−3.18

The velocity tensor is:

2.46	−1.99	0.26
−1.99	0.16	−0.12 mm/a
0.26	−0.12	−0.48

and in the eigensystem configuration we have:

v (mm/a)	Azimuth°	Plunge°
4.06	141	−4
−0.03	52	8
−0.51	28	−81

The results show that this belt is dominated by an extensional deformation at an average rate of 2.9±1.1 mm/a in a mean direction of N145°±4°E. It is interesting to note that this direction is almost the same with that in the volcanic arc.

Belt 8: Chios, Lesbos and central western Turkey

It includes zones 13 and 14b. Twelve fault plane solutions are used in the calculations listed with numbers 23, 24, 25, 27, 32, 33, 35, 36, 37, 42, 43 and 59 in Table 2, which show normal faulting. The components of the tensor $\bar{F}$ for this belt are as follows:

0.84	0.15	−0.42
0.15	0.02	−0.06
−0.42	−0.06	−0.86

Zone 13: This zone is located along the island of Chios and central Turkey. The strain rate tensor is:

1.60	0.28	−0.81
0.28	0.04	-0.12×10^{-8}/a
−0.81	−0.12	−1.63

The velocity tensor is:

1.71	0.75	−0.24
0.75	0.29	−0.04 mm/a
−0.24	−0.04	−0.25

The eigenvectors are:

v (mm/a)	Azimuth°	Plunge°
2.05	23	−6
−0.01	112	13
−0.28	136	−75

Zone 14b: This zone is located along the island of Lesvos and central Turkey. The strain rate tensor is as follows:

3.02	0.53	−1.53
0.53	0.07	-0.23×10^{-8}/a
−1.53	−0.23	−3.09

The velocity tensor is:

2.56	0.87	−0.46
0.87	0.24	−0.07 mm/a
−0.46	−0.07	−0.46

and in terms of eigenvectors we have:

v (mm/a)	Azimuth°	Plunge°
2.91	18	−8
−0.03	107	9
−0.54	149	−78

It is seen that the deformation is taken up by extension with an average velocity of 2.5±0.4 mm/a in a mean direction N20°±3°E. It is observed that the trend of the extensional field exhibits an eastward declination in comparison with the one of the southwestern Turkey.

Belt 9: northern Anatolia

It includes seismic zone 15 which extends along the westernmost end of the North Anatolian fault. The North Anatolian fault zone is a 1500 km long seismically active right lateral strike–slip fault that takes up the relative motion between the Anatolian block and Black Sea plate. This fault extends from the Karliova triple junction (41°E) as far as the Northern Aegean. Five fault plane solutions were used for the determination of what we call "shape" of the deformation, listed with numbers 3, 5, 22, 73 and 81 in Table 2. The components of the tensor $\bar{F}$ are as follows:

0.78	0.52	0.13
0.52	−0.45	−0.33
0.13	−0.33	−0.34

Zone 15: The strain rate tensor for this zone is:

8.32	5.58	1.43
5.58	−4.75	-3.51×10^{-8}/a
1.43	−3.51	−3.58

while the velocity tensor is:

11.75	15.84	0.43
15.84	−14.54	−1.05 mm/a
0.43	−1.05	−0.54

and in terms of eigenvectors we have:

v (mm/a)	Azimuth°	Plunge°
−22.04	115	3
19.19	25	0
−0.48	118	−87

It is seen that the deformation of this area is performed by compression at a rate of 22.0 mm/a in a direction N115°E direction, which is taken up by extension of 19.2 mm/a in a N25°E direction.

Belt 10: northern Aegean

It includes zone 14a and 16. Eight fault plane solutions were used, listed with numbers 6, 14, 17, 49, 67, 68, 69, 74 in Table 2, which mainly show strike–slip faulting. The tensor $\bar{F}$ is as follows:

0.81	−0.11	−0.03
−0.11	−0.76	0.09
−0.03	0.09	−0.05

Zone 14a: The strain rate tensor is:

4.89	−0.67	−0.20
−0.67	−4.58	0.55×10^{-8}/a
−0.20	0.55	−0.30

The velocity tensor is:

6.41	−0.37	−0.06
−0.37	−1.00	0.16 mm/a
−0.06	0.16	−0.05

and the eigensystem configuration is:

v (mm/a)	Azimuth°	Plunge°
−10.00	89	−1
6.42	179	1
−0.04	58	89

Zone 16: The strain rate tensor for this zone is:

13.10	−1.80	−0.52
−1.80	−12.29	1.47×10^{-8}/a
−0.52	1.47	−0.81

The velocity tensor is:

9.68	−1.62	−0.16
−1.62	−22.04	0.44 mm/a
−0.16	0.44	−0.12

while its eigenvectors are:

v (mm/a)	Azimuth°	Plunge°
9.77	177	1
−22.12	87	−1
−0.12	44	88

The continuation of the Northern Anatolian fault zone into the Aegean strongly controls the deformation pattern of the area. The right lateral motion of the fault which terminates abruptly in the North Aegean trough causes EW compression which reduces from 22.1 mm/a in zone 16 to 10.0 mm/a in zone 14a. The extension rate reduces from 9.8 mm/a in the eastern part (zone 16) to 6.4 mm/a in the western part of the belt (zone 14a).

Belt 11: central Macedonia–southern Bulgaria

It includes seismic zones 17, 18 and 19. Five fault plane solutions were used in the calculations, listed with numbers 2, 54, 55, 79 and 80 in Table 2. It is seen that there is a lack of focal mechanisms for zone 18. No reliable fault plane solution for any event with $M_s \geq 5.5$ is available for this zone. However, *in situ* stress measurements in this area (Paquin *et al.*, 1982) and macroseismic field simulation of the recent event of November 9, 1985, $M_s=5.5$ (Papazachos, 1992), clearly indicate an almost NS extensional pattern. The tensor $\bar{F}$ for the whole belt has as follows:

0.98	−0.04	−0.00
−0.04	−0.02	0.03
−0.00	0.03	−0.96

Zone 17: This zone is located in the Serbomacedonian massif. The most recent events in this area are those of the 1978 Thessaloniki sequence ($M_s=6.5$). The strain rate tensor is as follows:

16.17	−0.06	−0.00
−0.06	−0.32	0.48×10^{-8}/a
−0.00	0.48	−15.85

The velocity tensor is:

11.18	−3.81	−0.00
−3.81	0.90	0.14 mm/a
−0.00	0.14	−2.38

and in terms of eigenvectors we have:

v (mm/a)	Azimuth°	Plunge°
12.44	162	0
−0.35	72	4
−2.39	74	−86

Zone 18: This zone has a low seismicity level. The strain rate tensor is:

6.57	−0.03	−0.00
−0.03	−0.13	0.19×10^{-8}/a
−0.00	0.19	−6.44

The velocity tensor is:

2.65	−0.51	−0.00
−0.51	−0.13	0.06 mm/a
−0.00	0.06	−0.97

and in terms of eigenvectors we have:

v (mm/a)	Azimuth°	Plunge°
2.74	170	0
−0.22	80	4
−0.97	82	−86

Zone 19: This zone is located in southern Bulgaria. The strain rate tensor is:

7.70	−0.03	−0.00
−0.03	−0.15	0.23×10^{-8}/a
−0.00	0.23	−7.55

The velocity tensor is:

3.06	0.25	−0.00
0.25	−0.28	0.07 mm/a
−0.00	0.07	−1.13

The eigensystem configuration is:

v (mm/a)	Azimuth°	Plunge°
3.08	4	0
−0.30	94	5
−1.14	94	−85

As is seen, the deformation in southern Bulgaria and Thrace is performed as NS extension (N177°±7°E) at a rate of 2.96±0.2 mm/a. In central Macedonia (Thessaloniki region), however, the extension increases to 12.4 mm/a and its direction is N162°E.

4. DISCUSSION AND CONCLUSIONS

In the present paper the rates of crustal deformation in the Aegean and the surrounding area are calculated. The data analysis followed is taken from Papazachos and Kiratzi (1993). However, we would like to add a few comments to this procedure.

The calculation of a uniform $\bar{F}$ for a whole belt and its use in each zone belonging to that belt, obviously introduces a kind of smoothing to the deformation pattern within this belt. This is inevitable in the majority of cases due to the lack of enough focal mechanisms in each zone which could be used for a detailed calculation of its deformation. Moreover, unification of seismic zones in broader belts was also performed on the basis of similarity of the focal mechanisms. This similarity was checked in the following way: from equation (4) it is clear that if all fault plane solutions within a belt are identical then the eigenvalues of $\bar{F}$ should be 1, 0 and -1. Hence, the deviation of the eigenvalues of $\bar{F}$ from

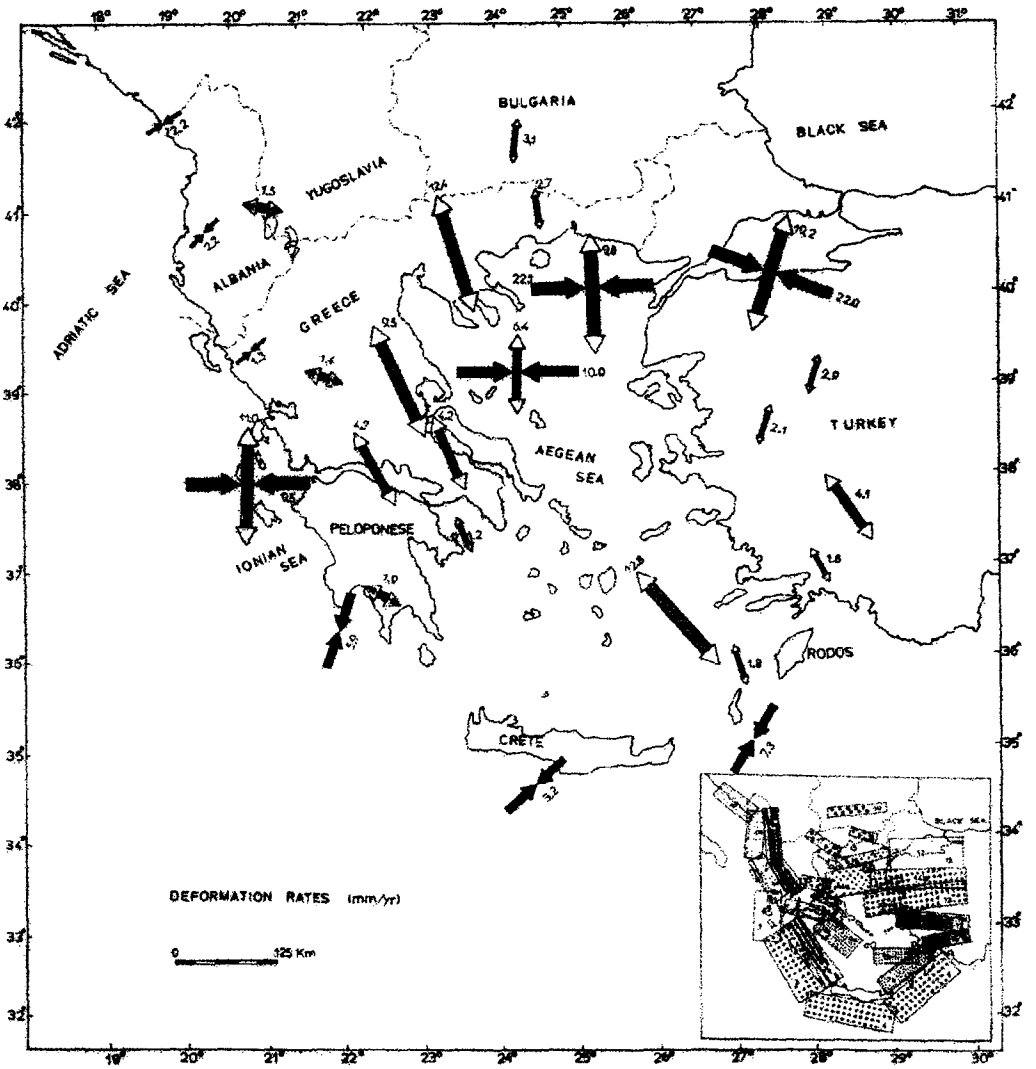

Fig. 4. Graphic representation of the pattern of deformation (in terms of velocity rates in mm/a) for the broader Aegean and surrounding area. The divergent arrows show extension while the convergent one show compression. The length of the arrows is indicative of the magnitude of the velocity rate. The inset figure shows the belts where the different zones have been grouped.

these values is a measure of the similarity of the fault plane solutions (specifically, of the P, T and null axis) for each belt. For the eleven belts (1,2,...11) the maximum eigenvalues of $\bar{F}$ (corresponding to T-axis) were 1, 0.9, 1, 1, 0.9, 1, 0.9, 1, 1, 0.8 and 1, while the minimum eigenvalues (corresponding to P-axis) were -1, -1, -0.9, -1, -0.9, -1, -0.9, -0.8, -1, respectively. The eigenvalues corresponding to the null axis were all smaller than 0.1. These results justify our assumption that all fault plane solutions used for each belt are very similar.

A crucial point for the calculation of the deformation is the estimation of $\dot{M}_0$, especially when historical data are used. In order to test the effect of historical seismicity and of the time period used for the calculation of $\dot{M}_0$ we reapplied the same method for its estimation [equation (1)] using initially all the instrumental data (after 1911) and afterwards only the most recent data (after 1950). As the time period in study diminishes, the $\dot{M}_0$ also has a tendency to decrease, especially in the low seismicity zones. This is expected since the largest events of such a zone might not occur during a 50 or even 100 year period. The importance of historical seismicity in low seismicity zones is critical, e.g. in zone 18 where only one major event with M_s=5.5 occured since 1911 (instrumental data). However, the same zone exhibits significant seismicity in the past century (e.g. 5 May 1829, M_s=7.3, I_0=X; 30 March 1867, M_s=6.0, I_0=VIII). If this seismicity is not taken into account a completely biased estimation of $\dot{M}_0$ and therefore of the deformation rates could be derived.

An important aspect of the whole procedure applied in the present paper is that of the accuracy of the results. Papazachos and Kiratzi (1993) performed a crude Monte Carlo simulation and showed that errors in strain rate and velocity tensors are mainly controlled by errors in the $\dot{M}_0$ assessment. They found that errors in $\dot{M}_0$ (and therefore in $\dot{\varepsilon}$ and U) due to errors in a, b, c, d and $M_{s,\,\max}$ [see equations (1), (2) and (3)] can account for an error factor up to about 3. However, errors in $\dot{M}_0$ have no effect on the direction of the eigenvector of deformation. This part of the results is influenced only by $\bar{F}$ and this is mainly controlled by the focal mechanisms of the large earthquakes.

Figure 4 is a map which graphically illustrates the maximum velocity rates, as they are obtained by the eigensystem of the velocity matrix, in the Aegean and the surrounding area. The length of the arrows is proportional to the magnitude of the velocity rates, while the absolute values of the velocities are written next to each arrow.

The following major patterns of deformation can be identified in the Aegean and its surrounding regions.

(1) Seismic shortening, due to continental collision, occurs along the coast of Yugoslavia, Albania and northwestern Greece, at a rate of the order of 2 mm/a.

(2) Horizontal seismic shortening occurs along the shallow seismogenic layer of the convex side of the Hellenic arc at an average rate of 5.5 mm/a in a direction N214°E. This rate of shortening, however, is by far less than the shortening rate calculated from plate motions which is considered to be of the order of 50–62 mm/a (Jackson and McKenzie, 1988b). In a recent work (Kiratzi and

Papazachos, 1992) it was found that the shallow part of the Benioff zone (defined by the foci in the depth range of 40–100 km) is shortened at a rate of about 20 mm/a, parallel to the strike of the arc and is extended at a rate of about 10 mm/a normal to the strike of the arc. If this shortening is the result of distributed deformation due to the subduction, then there is no good reason to believe that the deformation in the Hellenic arc is expressed aseismically.

The region of Ionian islands has the characteristics of a transform zone and represents the northwestern termination of the Hellenic subduction. Deformation is expressed as seismic shortening in an approximately EW direction at a slip rate of 11 mm/a and as extension at a rate of 10 mm/a in an about NS direction.

(3) Seismic extension in a more or less NS direction dominates in the back-arc Aegean area (except for the Northern Aegean trough and northwestern Anatolia fault zone). There is, however, some tendency for the extensional field to have some declination to the west in the mainland of Greece, in the southern Aegean volcanic arc and in southwestern Turkey and to the east in northwestern Turkey. The extension rate in this back-arc area varies from zone to zone (from 1 to 13 mm/a) and its average value is 5 mm/a. Geodetic observations revealed an average extension rate of about 11 mm/a in the direction 210° (Billiris *et al.*, 1991). It is evident that the seismicity of the back-arc Aegean area can account, within error limits, for at least 50% of this deformation.

(4) Deformation in the northwestern Anatolia is expressed as compression at a rate of 22 mm/a in a N115°E direction and as extension at a rate of 19 mm/a in a direction N25°E. The average compression in the North Aegean fault zones is 16 mm/a in a N88°E direction and the average extension is 8 mm/a in a N178°E direction.

(5) A belt between the external compressional area and the inner extensional one shows extension in an about EW direction. It includes eastern Albania, the western mainland of Greece and possibly extends up to the western corner of Crete. The extension rate is 1.6 mm/a in a direction N112°E.

(6) The component U_{33} of the velocity matrix gives the vertical thickening (positive values) or the vertical thinning (negative values) of the seismogenic layer. From the values of this component we see that the crust of the external zones (1a, 1b,...,5) is thickening at an average rate of 0.3 ± 0.1 mm/a, while the crust in the back-arc Aegean area (zones 7b, 8a, ...,19) is thinning at an average rate of 0.8 ± 0.7 mm/a. Neotectonic observations in the area of central Greece support this conclusion (Jackson *et al.*, 1982).

REFERENCES

Aki K. and Richards P. (1980) *Quantitative Seismology: Theory and Methods.* Freeman, San Francisco, CA.

Ambraseys N. N. and Jackson J. A. (1990) Seismicity and associated strain of central Greece between 1890 and 1988. *Geophys. J. Int.* **101**, 663–709.

Anderson H. and Jackson J. (1987) Active tectonics of the Adriatic Region. *Geophys. J. R. astr. Soc.* **91**, 937–983.

Billiris H., Paradisis D., Veis G., England P., Featherstone W., Parsons B., Cross P., Rands P., Rayson M., Sellers P., Ashkenazi V., Daivson M., Jackson J. and Ambraseys N. (1991) Geodetic determination of tectonic deformation in central Greece from 1900 to 1988. *Nature* **305**, 124–129.

Boore D., Sims J., Kanamori H. and Harding S. (1981) The Montenegro, Yugoslavia, earthquake of April 15, 1979: source orientation and strength. *Phys. Earth & Planet Interior* **27**, 133–142.

Comninakis P. and Papazachos B. (1986) A catalogue of earthquakes in the Aegean and surrounding area for the period 1901–1985. *Publ. of the Geophys. Lab., University of Thessaloniki* **1**, 167 pp.

Dziewonski A., Franzen J. and Woodhouse J. (1984) Centroid-moment tensor solutions for July–September, 1983. *Phys. Earth & Planet. Interiors* **34**, 1–8.

Ekstrom G. and England P. (1989) Seismic strain rates in regions of distributed continental deformation. *J. Geophys. Res.* **94**, 10231–10257.

Eyidogan H. (1988) Rates of crustal deformation in western Turkey as deduced from major earthquakes. *Tectonophysics* **148**, 83–92.

Hatzfeld D., Pedotti G., Hatzidimitriou P. and Makropoulos K. (1990) The strain pattern in the western Hellenic arc deduced from a microearthquake study. *Geophys. J. Int.* **101**, 181–202.

Jackson J. and McKenzie D. (1988a) The relationship between plate motions and seismic moment tensors, and the rates of active deformation in the Mediterranean and Middle East. *Geophysical J.* **93**, 45–73.

Jackson J. and McKenzie D. (1988b) Rates of active deformation in the Aegean Sea and surrounding regions. *Basin Res.* **1**, 121–128.

Jackson J., King G. and Vita-Finzi C. (1982) The neotectonics of the Aegean: an alternative view. *Earth Planet. Sci. Lett.* **61**, 303–318.

Ioannidou E. (1989) Seismic source parameters determined by the inversion of body waves: Greece and the surrounding area. Ph.D., thesis, University of Athens, pp. 185.

Kiratzi A. (1991) Rates of crustal deformation in the north Aegean trough-north Anatolian fault deduced from seismicity. *Pageoph* **136 (3)**, 421–432.

Kiratzi A. and Langston C. (1989) Estimation of earthquake source parameters of the May 4, 1972 event of the Hellenic arc by the inversion of waveform data. *Phys. Earth & Planet. Interiors* **57**, 225–232.

Kiratzi A. and Langston C. (1991) Moment tensor inversion of the 1983 January 17 Kefallinia event of Ionian islands (Greece). *Geophys. J. Int.* **105**, 529–535.

Kiratzi A. and Papazachos C. (1992) Active deformation in the southern Aegean Benioff zone. *Publ. Geophys. Lab. Univ. of Thessaloniki* **10**, 1–19.

Kiratzi A., Wagner G. and Langston C. (1991a) Source parameters of some large earthquakes in northern Aegean determined by body waveform inversion. *Pageoph* **135**, 515–527.

Kiratzi A., Papadimitriou E. and Papazachos B. (1991b) Seismic moments and focal depths of the earthquakes of the Aegean area determined by waveform modeling. *Publ. Geophys. Lab. Univ. of Thessaloniki* **10**, 1–14.

Kostrov V. (1974) Seismic moment and energy of earthquakes, and seismic flow of rock. *Izv. Acad. Sc. USSR Phys. Solid Earth* **1**, 23–44.

Liotier Y. (1989) Modelisation des ondes de volume ses seismes de l' arc Egeen. Formation de 3^{e} Cycle, UFR de Mechanique, Universite Joseph Fourier de Grenoble 1.

Lyon-Caen H. *et al.* (1988) The 1986 Kalamata (south Peloponnesus) earthquake: detailed study of a normal fault, evidence for east–west extension in the Hellenic arc. *J. geophys. Res.* **93**, 14967–15000.

McKenzie D. (1972) Active tectonics of the Mediterranean region *Geophys. J. R. astr. Soc.* **30**, 109–185.

McKenzie D. (1978) Active tectonics of the Alpine–Himalayan belt: the Aegean Sea and surrounding regions. *Geophys. J. R. astr. Soc.* **55**, 217–254.

Milne W. and Davenport A. (1969) Determination of earthquake risk in Canada. *Bull. seism. Soc. Am.* **59**, 729–754.

Molnar P. (1979) Earthquake recurrence intervals and plate tectonics. *Bull. seism. Soc. Am.* **69**, 115–133.

Papadimitriou E. E. (1992) Focal mechanisms along the convex side of the Hellenic Arc and its tectonic significance. *Publ. Geophys. Lab. Univ. of Thessaloniki* **8**, 1–20.

Papazachos B. (1990) Seismicity of the Aegean and surrounding area. *Tectonophysics* **178**, 287–308.

Papazachos B. and Papazachou C. (1989) *The Earthquakes of Greece.* Ziti Publication Company, Thessaloniki.

Papazachos B. and Panagiotopoulos D. (1993) Normal faults associated with volcanic activity and deep rupture zones in the southern Aegean volcanic arc. *Tectonophysics* (in press).

Papazachos B., Panagiotopoulos D., Tsapanos Th., Mountrakis D. and Dimopoulos G. (1983) A study of the 1980 summer seismic sequence in the Magnesia region of central Greece. *Geophys. J. R. astr. Soc.* **75**, 155–168.

Papazachos B., Kiratzi A., Hatzidimitriou P. and Rocca A. (1984a) Seismic faults in the Aegean area. *Tectonophysics* **106**, 71–85.

Papazachos B., Kiratzi A., Voidomatis Ph. and Papaioannou Ch. (1984b) A study of the December 1981–January 1982 seismic activity in northern Aegean Sea. *Boll. Geofis. Teor. Appl.* **26**, 101–102.

Papazachos B., Kiratzi A., Karacostas B., Panagiotopoulos D., Scordilis E. and Mountrakis D. (1988) Surface fault traces, fault plane solution and spatial distribution of the aftershocks of the September 13, 1986 earthquake of Kalamata (southern Greece). *Pageoph* **126**, 55–68.

Papazachos B. C., Kiratzi A. A., Papaioannou Ch. A. and Panagiotopoulos D. G. (1991a) Average regional seismic strain release rates in the Patraikos–Saronikos gulfs (central Greece) based on historical and instrumental data. *Bull. Geol. Soc. Greece* **XXV (3)**, 225–238.

Papazachos B. C., Kiratzi A. A. and Papadimitriou E. (1991b) Fault plane solutions for earthquakes in the Aegean area. *Pageoph* **136**, 405–420.

Papazachos C. (1992) Anisotropic radiation modelling of macroseismic intensities for estimation of the attenuation structure of the upper crust in Greece. *Pageoph* **138(3)**, 445–469.

Papazachos C. and Kiratzi A. (1993) A formulation for reliable estimation of active crustal deformation and its application to central Greece. *Geophys. J. Int.* (in press).

Paquin C., Froidevaux C., Ployet J., Ricard Y. and Angelidis C. (1982) Tectonic stresses on the mainland of Greece: in-situ measurements by overcoring. *Tectonophysics* **86**, 17–26.

Ritsema A. (1974) The earthquake mechanisms of the Balkan region. *R. Netherl. Meteorol. Inst., De Bilt, Sci. Rep.* 74–4.

Rocca A., Karakaisis G., Karacostas B., Kiratzi A., Scordilis E. and Papazachos B. (1985) Further evidence on the strike slip-faulting of the northern Aegean trough based on properties of the August–November 1983 seismic sequence. *Boll. di Geof. Teor. ed Appl.* **27**, 101–109.

Scordilis E., Karakaisis G., Karacostas B., Panagiotopoulos D., Comninakis P. and Papazachos B. (1985) Evidence for transform faulting in the Ionian Sea: the Cephalonia island earthquake sequence of 1983. *Pageoph* **123**, 388–397.

Shirokova E. (1972) Stress pattern and probable motion in the earthquake foci of the Asia-Mediterranean seismic belt. In *Elastic Strain Field of the Earth and Mechanisms of Earthquake Sources* (Balakina L. M., *et al.*, eds), p. 8. Nauka, Moscow.

Soufleris Ch. and Stewart G. (1981) A source study of the Thessaloniki (N. Greece) 1978 earthquake sequence. *Geophys. J. R. astr. Soc.* **67**, 343–358.

Taymaz T., Jackson J. and Westaway R. (1990) Earthquake mechanisms in the Hellenic Trench near Crete. *Geophys. J. Int.* **102**, 695–731.

Taymaz T., Jackson J. and McKenzie D. (1991) Active tectonics of the north and central Aegean Sea. *Geophys. J. Int.* **106**, 433–490.

Tselentis G. and Makropoulos C. (1986) Rates of crustal deformation in the gulf of Corinth (central Greece) as determined from seismicity. *Tectonophysics* **124**, 55–66.

Tselentis G., Stavrakakis G., Makropoulos K., Latousakis J. and Drakopoulos J. (1988) Seismic moments of earthquakes at the western Hellenic arc and their application to the seismic hazard of the area. *Tectonophysics* **148**, 73–82.